ANCIENT VOLCANISM MAY HAVE INFLUENCED PATTERNS OF HYDRATED REGOLITH ON MARS. T.G. Paladino[1], S.E.K. Nawotniak[1], L. Kerber[2], E. Millour[3], S. Karunatillake[4]. [1]Department of Geosciences, Idaho State University, Pocatello, ID 83204, USA (tylerpaladino@isu.edu), [2]Jet Propulsion Laboratory, Caltech, Pasadena, CA 91109, USA, [3]Laboratoire de Métérologie Dynamique, IPSL, Universite Pierre et Marie Curie, Paris 75005, France, [4]Department of Geology and Geophysics, Louisiana State University, Baton Rouge, LA 70803, USA.

Introduction: The Gamma Ray Spectrometer (GRS) instrument has shown regionally variable hydration in the upper decimeters of the martian regolith [1](fig.1c) that are difficult to explain. Current hypotheses, including dust cover variations, hydrous Fe-sulfates from acid fog leaching, and hydrous alteration may all contribute to these patterns. Here we introduce explosive volcanism in an ancient martian atmosphere as a possible mechanism to produce these hydration patterns in addition to the above hypotheses.

Explosive Volcanism to Hydrated Regolith: Ash derived from explosive volcanism is capable of being hydrated through two main pathways. The first is post-eruptive. After being deposited, ash acts much like a sponge over geologic timescales where it can absorb water as it transitions into hydrated clays [2,3]. The second pathway for ash hydration is syn-eruptively during a phreatic or phreatomagmatic eruption [4,5] in a particularly wet environment. Because ash in a thick martian atmosphere is capable of being transported 100s of kilometers from its eruptive source [6], a mechanism exists to transport or absorb water throughout the surface of the planet via explosive volcanism either post- or syn-eruptively.

Modeling Workflow: To test whether explosive volcanism has influenced observed patterns of regolith hydration, we adopt the following workflow using two models: the Active Tracer High-resolution Atmospheric Model (ATHAM [7]) and the Laboratoire de Météorologie Dynamique General Circulation Model (LMD GCM [8]). ATHAM simulates an explosive eruption plume in an atmosphere sourced from the LMD GCM for each season. The ash from these simulated plumes is then input back into the LMD GCM to track ash dispersion and deposition as a passive tracer over a martian year. This workflow is done for every volcano on Mars that shows evidence for explosive activity in the form of morphologic characteristics, geochemical considerations, and proximity to ash deposits [9].

Eruption and Atmospheric Characteristics: Every eruption was initialized with conditions summarized in table 1. ATHAM acts in a cartesian coordinate system with decreasing resolution away from the vent. The horizontal domain extent was 100 x 100 km and the vertical domain extent was 80 km. The atmosphere was modeled off the cold and dry scenario presented by Wordsworth et al. [11] at 1 bar surface pressure and modern-day obliquity. We chose to use a 1 bar atmosphere as all the explosive volcanoes modeled here were primarily active in the Noachian and Hesperian [12], when Mars had a thicker atmosphere.

Table 1: Input parameters for the plume model, ATHAM.

MER (kg/s)	6.65×10^6
Ash Density (kg/m^3)	700
Ash Temperature (K)	1450
Plume Water Content (%)	4
Grainsize Distribution	Unit 3 of the 25.4 ka Oruanui deposit [10]

For the same reason, the Tharsis Rise topography is also removed. The GCM was run on a 128x96x23 (lonxlatxalt) grid.

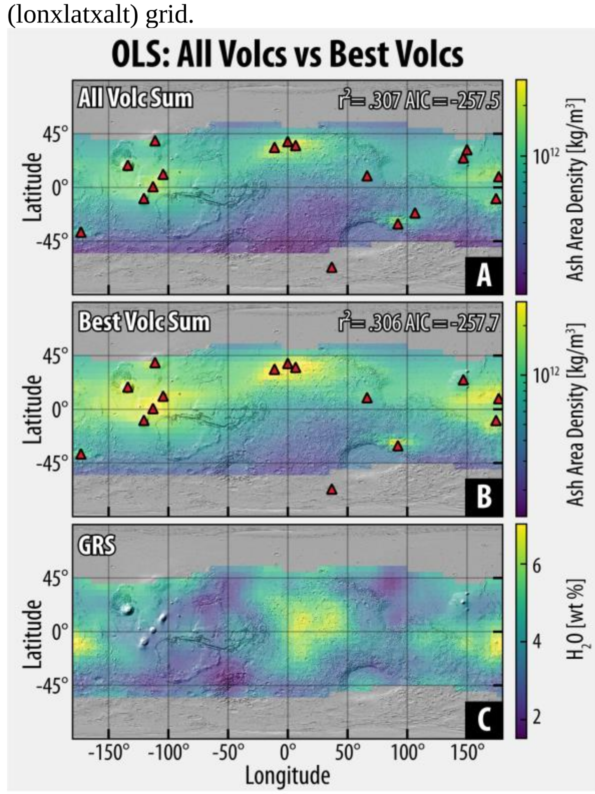

Figure 1: OLS results for all volcanoes (A), best volcanoes given by the lowest AIC value (B) and the GRS hydration data (C). A and B show summations of the modeled ash deposition from relevant volcanoes that were used in the OLS model.

Statistical Analysis: We use an ordinary least squares (OLS) regression model to test which combination of volcanoes provide the best fit with the GRS data. The modeled ash deposition and the GRS H2O data is transformed using a boxcox transformation to achieve linearity. Four volcanoes near or within the

Malea Planum region showed high degrees of autocorrelation with each other. OLS requires all predictive variables to not be correlated with each other, so 3 of these volcanoes with the largest variance inflation factors were removed from analysis (Malea, Peneus, and Amphirites Patera).

To find the combination of volcanoes that best predicts the GRS H2O data, we use the Akaike Information Criterion (AIC), which scores the quality of each model in comparison with each other. Lower AIC values indicate a simple, better-quality model. We then test all possible unique combinations (in this case, 2^{17}), and find the set with the lowest AIC value.

Results and Discussion: We first present the case of all volcanoes (with the exception of the Malea Planum volcanoes mentioned above) being used to predict the GRS data. By summing the ash deposition of these volcanoes together and displaying them next to the GRS data, we can gain a qualitative sense for how good of a fit all the volcanoes are with the GRS hydration data (fig. 1a). Running this combination through OLS gives an r^2 value of .307 and an AIC value of -257.5.

From considering the AIC criterion, we can find the highest quality OLS model of all possible combinations of volcanoes to compare with the every-volcano case. The best OLS model gives an AIC value of -257.7 and an r^2 value of .306 and yields a slightly different ash deposition map than from the every-volcano approach (fig. 1b). Contrasting the two scenarios yields fairly similar results, with AIC and r^2 values very close to each other.

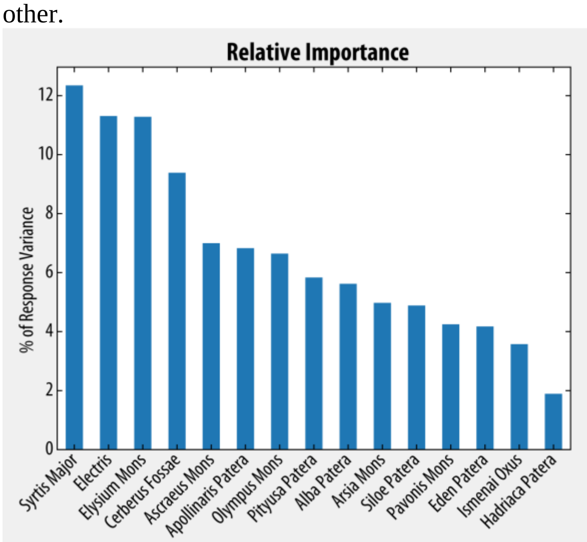

Figure 2: Relative importance of each predictor. This plot shows the percent of response variance for each predictor variable used in the best regression model, calculated using the methodology of Lindman et al. 1980 [13].

Observing the summed ash maps (fig. 1a-b), shows similar patterns of deposition. In both cases, the ash deposition matches well with hydrated area around 180° longitude and -5° latitude, as well as moderately hydrated areas around northern Tharsis or northeastern Hellas. The obvious feature missing is the high hydration zone within Terra Sabaea and northern Noachis Terra. The moderately hydrated areas in Arabia Terra are reasonably explained by the ash deposition data.

Relative Importance of Each Volcano: It is often useful to find the relative importance of each predictor. This can be done using the methodology of Lindeman et al. [13], in which predictors are added one at a time to the model to observe how the r^2 value changes. Because the order a new predictor being added influences the r^2 value, all possible orders are averaged. Using this methodology on the best AIC case gives figure 2. Volcanoes such as Sytris Major, Electris, Elysium Mons, and Cerberus Fossae have larger importance, while volcanoes in Arabia Terra (Siloe, Eden, and Ismenia), Hadriaca Patera, and some Tharsis volcanoes have low importance. Proximity of volcanoes to elevated hydration areas generally explain these trends.

Conclusions: From this analysis, we have found that volcanism may help explain patterns of hydrated regolith in addition to other hypotheses. By using two models to simulate martian climate and explosive plumes, then running results through an OLS model, we found the combination of volcanoes that best explain hydration patterns in GRS data.

Further Work: Moving forward, we will implement a more robust statistical regression methodology such as the hierarchical regression scheme put forth by Karunitallake et al. [14].

Acknowledgements: This work was supported by NASA MDAP grant 80NSSC18K1375. This research made use of the resources of the High Performance Computing Center at Idaho National Laboratory, which is supported by the Office of Nuclear Energy of the U.S. Department of Energy and the Nuclear Science User Facilities under Contract No. DE-AC07-05ID14517

References: **[1]** W. V. Boynton et al. (2007) JGR E: Planets. 112.12, pp. 1–15. **[2]** S. Aomine and K. Wada. (1962) Am. Mineral. 47, pp. 1024–1048. **[3]** A.P.W. Hodder et al. (1990) Clay Miner. 25, pp. 313–327. **[4]** M.R. Hudak et al. (2021). Geophys. Res. Lett. 48. **[5]** S.J. Mitchell et al. (2018) Earth Planet. Sci. Lett. 494, pp. 135–147. **[6]** L. Kerber et al. (2012) Icarus 219.1, pp. 358–381. **[7]** J.M. Oberhuber et al. (1998) J. Volcanol. Geotherm. Res. 87, pp. 29–53. **[8] F.** Forget et al. (1999) J. Geophys. Res. Planets 104, pp. 24155–24175. **[9]** P. Brož et al. (2021) J. Volcanol. Geotherm. Res. 409. **[10] S.** Self (1983) J. Volcanol. Geotherm. Res., Explosive Volcanism 17, pp. 433–469. **[11]** R.D. Wordsworth et al. (2015) J. Geophys. Res. Planets 120, pp. 1201–1219. **[12]** S.J. Robbins et al. (2011) Icarus 211, pp. 1179–1203. **[13]** R.H. Lindeman et al. (1980) **[14]** Karunatillake, S. et al. (2012) Earth Moon Planets 108, 253–273.